Available online at www.sciencedirect.com
ScienceDirect
Journal of Power Sources 159 (2006) 29–33
JOURNAL OF POWER SOURCES
www.elsevier.com/locate/jpowsour

Short communication

Multi-scale dispersion in fuel cell anode catalysts: Role of TiO_2 towards achieving nanostructured materials

Jiun-Ming Chen [a], Loka Subramanyam Sarma [a], Ching-Hsiang Chen [a], Ming-Yao Cheng [a], Shou-Chu Shih [a], Guo-Rung Wang [a], Din-Goa Liu [b], Jyh-Fu Lee [b], Mau-Tsu Tang [b], Bing-Joe Hwang [a,b,*]

[a] *Nanoelectrochemistry Laboratory, Department of Chemical Engineering, National Taiwan University of Science and Technology, Taipei 106, Taiwan, ROC*
[b] *National Synchrotron Radiation Research Center, Hsinchu 300, Taiwan, ROC*

Available online 14 June 2006

Abstract

Multi-scale dispersion involving dispersion of catalyst particles on carbon support as well as intra-particle dispersion within the particles of a ternary Pt-Ru-Ti/C catalyst has been demonstrated. The presence of TiO_2 can dramatically decreases the grain size of the obtained catalyst to about 1–2 nm when compared with similarly prepared Pt-Ru/C (3–4 nm) catalyst indicating that TiO_2 can enhance the dispersion of the catalyst particles on carbon support. The structure and distribution of the Pt-Ru-Ti/C catalyst nanoparticles has been studied from high angle annular dark-field (HAADF) images combining with energy-dispersive X-ray spectroscopy (EDX). The composition of the Pt–Ru–Ti/C was found to be 50:34:16 (Pt:Ru:Ti, at%). The role of TiO_2 in improving the intra-particle distribution has been investigated by X-ray absorption spectroscopy (XAS) at extended X-ray absorption fine structure region (EXAFS). The XAS parameters suggest that the Pt-Ru-Ti/C catalyst possess a structure in which the core is rich in Pt–Ru alloy and the shell is rich in Pt. In the shell, the Pt, Ru and TiO_2 species are distributed homogenously. As a result of the improved multi-scale dispersion, the Pt-Ru-Ti/C catalyst exhibited enhanced activity towards methanol oxidation when compared to the commercial E-TEK 30 Pt-Ru/C catalyst and shows nearly similar performance when compared to the commercial JM 30 Pt-Ru/C catalyst with promising applications in fuel cells.
© 2006 Elsevier B.V. All rights reserved.

Keywords: Multi-scale dispersion; Electrocatalysts; Titanium dioxide; EXAFS

1. Introduction

Highly dispersed and size selected nanoelectrocatalysts are currently in great demand to enhance the performance of direct methanol fuel cells (DMFCs) [1]. In general, most catalytic reaction activities are structure sensitive and this in turn depends on the achievement of multi-scale dispersion and stability of the catalyst particles. As the name implies, multi-scale dispersion involves the high dispersion of catalyst particles on the support as well as the intra-particle dispersion among the constituent elements and it has significant impact on the activity. By far the most common approach to prevent agglomeration and coalescence of the nanoparticles on fuel cell catalysts is through stabilizing them with surfactants such as polyvinyl pyrrolidine [2]. In order to allow the fuel access to the catalytic sites, the stabilization agent should be removed preferably by oxidative heat treatment [3]. However, heat treatment poses additional problems such as phase separation of active metals, coalescence of particles, and alteration of surface concentration of the catalyst [4]. With these existing difficulties, no significant progress has been achieved so far in effectively providing the intra-particle dispersion. Thus, there exists a great interest in improving the multi-scale dispersion in the catalysts and establishing its relationship with the activity of catalysts.

In this contribution, we demonstrate the multi-scale dispersion in a fuel cell anode catalyst Pt-Ru-Ti/C obtained by introducing TiO_2 into the Pt–Ru matrix when compared to the in-house prepared Pt-Ru/C, commercial E-TEK 30 and JM 30 Pt-Ru/C catalysts. The presence of TiO_2 in the Pt–Ru matrix

* Corresponding author. Tel.: +886 2 27376624; fax: +886 2 27376644.
E-mail address: bjh@mail.ntust.edu.tw (B.-J. Hwang).

0378-7753/$ – see front matter © 2006 Elsevier B.V. All rights reserved.
doi:10.1016/j.jpowsour.2006.04.135

likely to perform roles, such as (i) avoid the agglomeration of Pt–Ru particles, (ii) effectively disperse the Pt and Ru atoms in the clusters and (iii) control the nanostructure of the catalyst. Based on the X-ray absorption spectroscopic analysis, we have evaluated the structural parameters to understand the extent of atomic distribution of Pt and Ru species and attempted to establish its relationship to the superior activity of Pt-Ru-Ti/C catalyst. X-ray absorption spectroscopy (XAS) studies at extended X-ray absorption fine structure (EXAFS) region (above the edge, ~30–50 eV) has proved to be an invaluable tool for structural studies of the catalysts and has wide applications [5–8].

2. Experimental

2.1. Preparation of Vulcan XC-72 carbon-supported Pt-Ru-Ti alloy catalyst

The Pt-Ru-Ti/C catalyst was prepared by using a slight modification of colloidal reduction method originally developed to synthesize Pt-Ru/C catalysts by Watanabe et al. [9]. Two commercial Pt-Ru/C catalysts, one is a 20% Pt-10% Ru supplied by E-TEK and the other is a 20% Pt-10 % Ru supplied by Johnson–Matthey, both with a Pt/Ru atomic ratio of 1:1 and an average particle sizes of 2–3 nm, were also utilized for comparison study.

2.2. XAFS measurements and data analysis

The X-ray absorption spectra were recorded at the Beam Line BL12B2 at the Spring-8, Hyogo, Japan. The electron storage ring was operated at 8 GeV. Prior to the XAS measurements, the catalyst sample in the holder was treated with pure H_2 gas for 30 min with a flow rate of 30 cm^3 H_2 min^{-1}, and then performed the XAS scan. Standard procedures were followed to analyze the XAS data. The EXAFS function, χ, was obtained by subtracting the post-edge background from the overall absorption and then normalized with respect to the edge jump step. Subsequently, k^3-weighted $\chi(k)$ data in the k-space ranging from 3.6 to 12.5 $Å^{-1}$ for the Pt L_{III}-edge, from 3.6 to 11.6 $Å^{-1}$ for the Ru K-edge were Fourier transformed (FT) to r-space to separate the EXAFS contributions from the different coordination shells. A nonlinear least-squares algorithm was applied to the curve fitting of an EXAFS in the r-space between 1.7 and 3.2 Å (without phase correction) for Pt, between 1.5 and 3.3 Å for Ru. The Pt–Ru reference file was determined by a theoretical calculation. All the computer programs were implemented in the UWXAFS 3.0 package with the backscattering amplitude and the phase shift

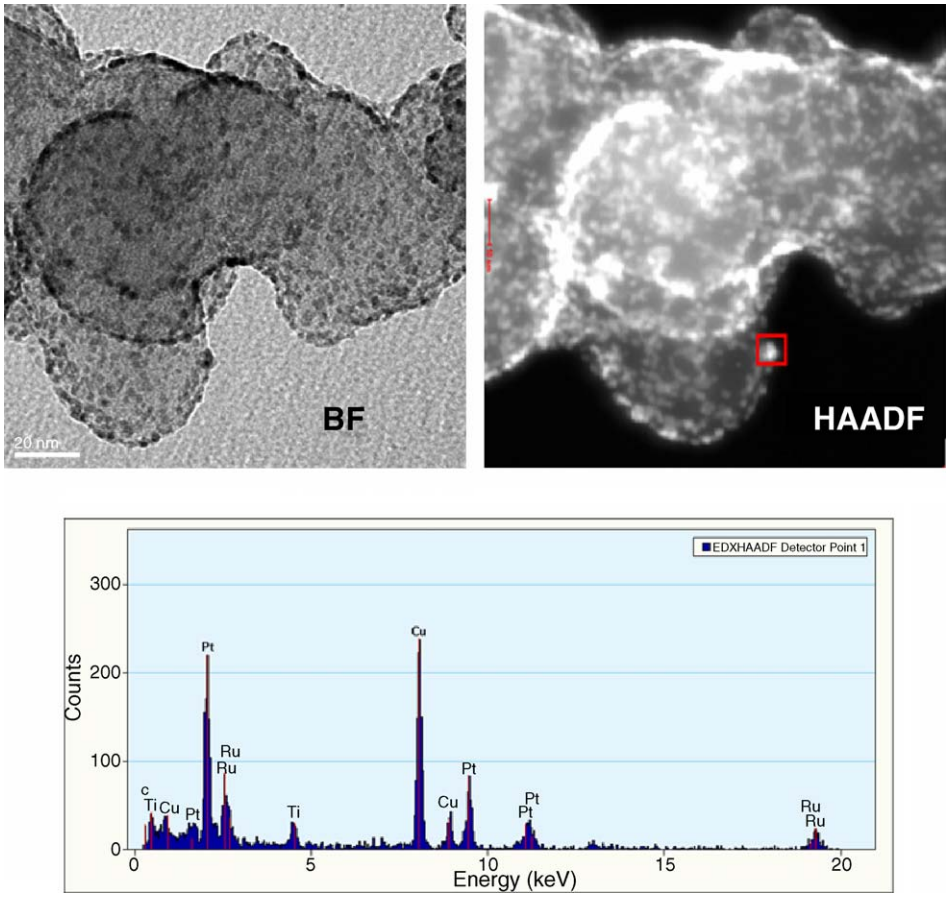

Fig. 1. Representative STEM bright field (BF) and HAADF images (×5,90,000, 200 kV) of the Pt-Ru-Ti/C catalyst nanoparticles and the corresponding EDX spectra (the beam location is illustrated in the HAADF image).

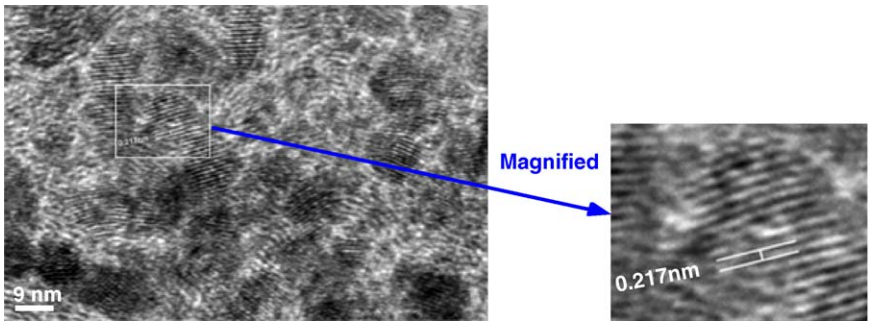

Fig. 2. HRTEM image of the Pt-Ru-Ti/C catalyst. The most prominent fringe index to $(1\,1\,1)_{FCC}$ (0.217 nm).

for the specific atom pairs being theoretically calculated by using FEFF7 code.

3. Results and discussion

The grain size for the in-house prepared Pt-Ru/C, Pt-Ru-Ti/C catalysts and commercial E-TEK 30 and JM 30 Pt-Ru/C are determined by Scherrer's equation using the (2 2 0) peak of their XRD patterns (data not shown here). The presence of TiO_2 in the catalyst matrix dramatically decreases the Pt-Ru-Ti/C grain size to about 1–2 nm when compared to the grain size of similarly prepared Pt-Ru/C catalyst (3–4 nm), indicating that TiO_2 enhances the dispersion of the catalyst particles on carbon support. In order to get additional insights in to the structure and distribution of the Pt-Ru-Ti/C catalyst, its high resolution TEM and HAADF images were obtained by using a FEI E.O Tecnai F20G2 MAT S-TWIN Field Emission Gun (FEG) (S) TEM apparatus operated at 200 kV. Representative bright field (BF) and HAADF images of the Pt-Ru-Ti/C electrocatalyst are shown in Fig. 1. The BF image shows that the catalyst particles are homogeneously supported with a high degree of dispersion on carbon. Comparison of HAADF image with BF image of Fig. 1 provides a better resolution which was due to the large difference in electron scattering between heavy metal nanoparticles and low-Z carbon support at high angles. The dimension of the metal nanoparticle in the synthesized Pt-Ru-Ti/C catalyst was checked with the previous results obtained by XRD. The aggregation of the metal nanoparticles at the edge was believed due to the 2D transmission electron image, which could be taken as the projection image of lateral side of the metal nanoparticles. Furthermore, the composition of the selected nanoparticle was determined by nanoprobe energy-dispersive X-ray analysis (EDX). Quantitative analysis of EDX spectra reveals a composition of 50 at% Pt, 34 at% Ru and 16 at% Ti in the irradiated Pt-Ru-Ti/C catalyst nanoparticle

Table 1
Results of EXAFS analysis for Pt-Ru-Ti/C (50:34:16), Pt-Ru/C, commercial E-TEK 30, and JM 30 Pt-Ru/C (50:50) catalysts

Catalyst	Bond	N	R (Å)	ΔE_0 (eV)	$\Delta\sigma_j^2 \times 10^{-3}$ (Å^2)	R-factor
Pt L_{III}-edge						
JM 30	Pt–Ru	1.4 (0.1)	2.700 (0.003)	4.5 (0.7)	2.4 (0.3)	0.0065
	Pt–Pt	5.6 (0.3)	2.734 (0.003)	4.2 (0.4)	5.5 (0.3)	
E-TEK 30	Pt–Ru	0.9 (0.1)	2.699 (0.004)	4.0 (1.0)	2.0 (0.4)	0.0053
	Pt–Pt	6.2 (0.3)	2.742 (0.002)	4.9 (0.4)	5.4 (0.2)	
Pt-Ru/C	Pt–Ru	1.2 (0.1)	2.701 (0.003)	4.8 (0.7)	1.9 (0.4)	0.0068
	Pt–Pt	5.9 (0.3)	2.730 (0.003)	3.6 (0.4)	5.7 (0.3)	
Pt-Ru-Ti/C	Pt–Ru	1.2 (0.03)	2.706 (0.001)	6.1 (0.24)	1.3 (0.13)	0.0007
	Pt–Pt	4.4 (0.09)	2.721 (0.001)	2.6 (0.22)	4.2(0.12)	
	Pt–Ti	0.6 (0.17)	2.359 (0.022)	−32.9 (4.13)	1.4(0.33)	
Ru K-edge						
JM 30	Ru–Pt	2.2 (0.3)	2.692 (0.007)	0.2 (1.0)	3.5 (0.8)	0.0081
	Ru–Ru	3.4 (0.2)	2.659 (0.003)	3.0 (0.4)	5.1 (0.4)	
E-TEK 30	Ru–Pt	1.2 (0.2)	2.691 (0.008)	0.7 (1.4)	1.0 (0.9)	0.0052
	Ru–Ru	3.7 (0.2)	2.663 (0.003)	4.6 (0.4)	4.3 (0.3)	
Pt-Ru/C	Ru–Pt	3.7 (0.3)	2.676 (0.005)	−4.6 (0.8)	4.3 (0.6)	0.0083
	Ru–Ru	3.2 (0.2)	2.662 (0.003)	4.4 (0.5)	3.9 (0.4)	
Pt-Ru-Ti/C	Ru–Pt	3.9 (0.5)	2.647 (0.006)	−12.2 (1.3)	4.0 (0.6)	0.0097
	Ru–Ru	3.5 (0.3)	2.654 (0.003)	1.5 (0.7)	3.7 (0.36)	
	Ru–Ti	0.1 (0.6)	2.453 (0.27)	4.2 (15.04)	2.7 (0.6)	

N, Coordination number; R, Bond distance; $\Delta\sigma_j^2$, Debye–Waller factor; ΔE_0, Inner potential shift.

(inside the square in the HAADF image of Fig. 1). The HRTEM image of the Pt-Ru-Ti/C catalyst sample was shown in Fig. 2. Lattice fringes of 0.20–0.23 nm corresponding to $Pt_{\alpha}Ru_{\beta}$ (1 1 1) are observed. Lattice fringes corresponding to hexagonal Ru are not observed. However, the grain size of the metal nanoparticle in HRTEM image seemed to be around 2 nm which is similar to the one obtained from XRD and HAADF image.

Evidence for the enhancement of intra-particle dispersion in the Pt-Ru-Ti/C catalyst comes from XAS experiments. The EXAFS spectra of the Pt L_{III}-edge and Ru K-edge for the studied electrocatalysts were obtained (data not shown here) and the corresponding fitting parameters, e.g., interatomic distance (R), coordination number (N) and Debye–Waller factor (σ_j^2) extracted from the EXAFS refinement are summarized in Table 1. At Pt L_{III}-edge, in all the catalyst, there appears splitting of a peak corresponding to the first coordination shell in the region 1.8–3.2 Å caused by the EXAFS contributions from Pt–Pt and Pt–Ru shells and this has been ascribed to the formation of Pt–Ru nanoparticles [10–12]. The coordination number of scattering Ru atoms around adsorbing Pt atoms ($N_{Pt–Ru}$) is found to be increased in the case of ternary Pt-Ru-Ti/C compared to the E-TEK 30 Pt-Ru/C catalyst. We believe that the presence of TiO_2 could influence the morphology of the catalyst by effectively dispersing the Pt and Ru atoms in the catalytic clusters and increased the $N_{Pt–Ru}$. Herein, we have attempted to probe how TiO_2 enhances the intra-particle dispersion among Pt and Ru atoms by constructing structural models for the catalysts based on calculated XAS parameters. We have calculated the ratio of the scattering 'Ru' atoms coordination number around absorbing 'Pt' atoms ($N_{Pt–Ru}$) to the total coordination number of absorbing atoms ($A = \Sigma N_{Pt–i}$) and represented as "($P = N_{Pt–Ru}/\Sigma N_{Pt–i}$)". In a similar manner the ratio of the scattering 'Pt' atoms coordination number around absorbing 'Ru' atoms ($N_{Ru–Pt}$) to the total coordination number of absorbing atoms ($B = \Sigma N_{Ru–i}$) has been calculated and represented as "($R = N_{Ru–Pt}/\Sigma N_{Ru–i}$)" and presented in Table 2. It is possible to estimate the intra-particle dispersion within the catalyst particles with the knowledge of the structural parameters P, R, A and B [13].

Based on the XAS parameters, it is found that $A > B$ and $R > P$ in the case of E-TEK 30, JM 30 and in-house prepared Pt-Ru/C catalyst, indicating a Pt-rich core surrounded by a shell enriched in Ru. The observed parameter relationship i.e. $A > B$ is consistent with the relationship $N_{AA} + N_{AB} > N_{BA} + N_{BB}$ for a homogeneous system for which the core of the cluster is composed of N atoms of A (N_A) and the surface is made of N atoms of B (N_B), the total coordination number ($N_{AA} + N_{AB}$) for the 'A' atom and greater than the total coordination for the 'B' atoms ($N_{BA} + N_{BB}$). The structural parameters P and R in the case of E-TEK 30 calculated as 0.13 and 0.24, respectively, and in the case of JM 30 these values are found to be 0.20 and 0.39, respectively. The progressive increase in P and R values can be taken as an indication of increasing the extent of intra-particle dispersion. In E-TEK 30 segregation of Pt and Ru atoms is serious in the core and shell, respectively, and hence small extent of intra-particle dispersion is obtained as lower number of P and R values suggests. Recent infrared measurements on the Pt–Ru alloy particle electrodes indicates two modes of adsorbed CO vibrations related to both Pt and Ru domains present on the surface supports the surface segregation of Ru in commercial catalysts [14]. The increased P and R values in the case of JM 30 suggest that the segregation of Pt and Ru atoms is not serious so as to achieve improved intra-particle dispersion. In the case of ternary Pt-Ru-Ti/C ($A < B$ and $P < R$), the catalyst adopts an inverted structure in which Pt is rich in the shell and Pt–Ru alloy rich in the core. However, the extent of segregation of Pt and Ru atoms is much less, as suggested by the increase in P and R values, due to the significant role of TiO_2 in enhancing the dispersion of the Pt and Ru atoms in the catalyst clusters and improving the intra-particle dispersion (Fig. 3).

Table 2
Structural coordination parameters for in-house prepared Pt-Ru/C, Pt-Ru-Ti/C, and commercial E-TEK 30 and JM 30 Pt-Ru/C (50:50) catalysts.

Catalyst	P	R	A	B
JM 30 Pt-Ru/C	0.20	0.39	7.0	5.6
E-TEK 30 Pt-Ru/C	0.13	0.24	7.1	4.9
Pt-Ru/C (in-house prepared)	0.17	0.54	7.1	6.9
Pt-Ru-Ti/C (in-house prepared)	0.21	0.53	5.6	7.4

The CO stripping voltammograms recorded on commercial E-TEK 30, JM 30 Pt-Ru/C catalysts and in-house prepared Pt-Ru-Ti/C catalysts are shown in Fig. 4. The current has been normalized to the electrochemically active noble metal surface area (A_{act}) which was obtained from the experimentally observed

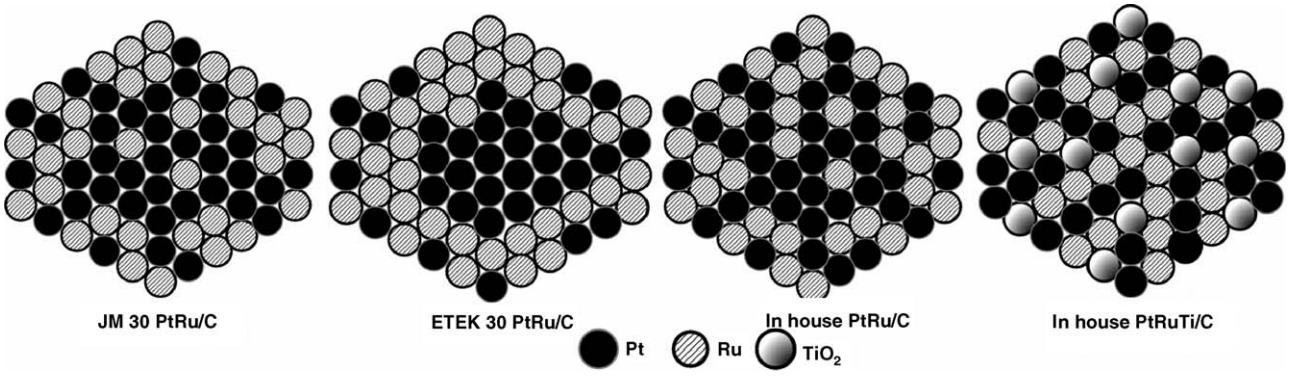

Fig. 3. Schematic presentation of the structures of JM 30, E-TEK30 Pt-Ru/C catalysts, and in-house prepared Pt-Ru/C and Pt-Ru-Ti/C catalysts.

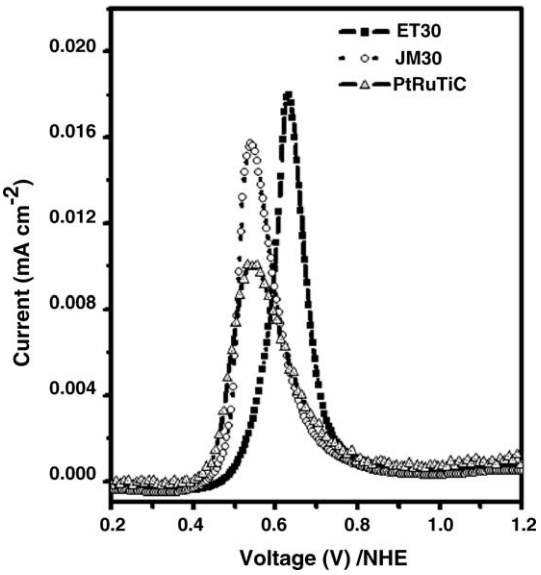

Fig. 4. CO stripping voltammograms recorded at 5 mV s^{-1} in 0.5 M H_2SO_4 solution for the prepared Pt-Ru-Ti/C, E-TEK 30 and JM 30 Pt-Ru/C catalysts (CO gas was purged for 15 min at 0.1 V vs. NHE and then stripped). Current has been normalized to electrochemical active surface area of Pt.

CO stripping charges (area of the stripping peak divided by the scan rate) divided by the charge required to oxidize a monolayer of linearly adsorbed CO on Pt (420 μC cm^{-2}) [15].

The onset potential of the adsorbed CO increases in the following order: Pt-Ru-Ti/C (ca. 0.37 V) < JM 30 Pt-Ru/C (ca. 0.39 V) < E-TEK 30 Pt-Ru/C (ca. 0.44 V). The presence of Ti appears to aid in the oxidation of CO at lower potentials. The role of Ti in terms of electronic and bifunctional effects is of particular importance and will be addressed in our future papers. It is seen that the CO stripping peak potential values are in the following order: Pt-Ru-Ti/C (ca. 0.54 V) ≈ JM 30 Pt-Ru/C (ca. 0.54 V) < E-TEK 30 Pt-Ru/C (0.63 V). Compared to the CO stripping peak potential of polycrystalline Pt (≈0.72 V) [16],the Pt-Ru-Ti/C catalyst shows the catalytic enhancement towards CO oxidation in the order of 0.18–0.26 V.

Chronoamperometric analysis at constant potential of 0.5 V versus NHE recorded on the catalysts in 15% CH_3OH + 0.5 M H_2SO_4 indicated that the Pt-Ru-Ti/C catalyst performs well over the E-TEK 30 and Pt-Ru/C catalysts. The segregation of Ru in the case of E-TEK 30 in part may be responsible for its lower methanol oxidation activity compared to JM 30 [13]. When compared to the commercial JM 30 Pt-Ru/C the prepared Pt-Ru-Ti/C catalyst shows slightly improved performance. Improved multi-scale dispersion in Pt-Ru-Ti/C catalyst can be attributed to its enhanced performance towards methanol oxidation.

4. Conclusion

In conclusion, one can achieve multi-scale dispersion in catalysts by introducing TiO_2 in the catalyst matrix. TiO_2 can disperse well the Pt and Ru atoms in the catalyst clusters and also disperse nanoparticles well on to carbon. The E-TEK 30, JM 30 and in-house prepared Pt-Ru/C catalysts adopts Ru rich in shell and Pt rich in core structure, whereas Pt-Ru-Ti/C adopts an inverted structure in which Pt rich in shell and Pt–Ru alloy rich in the core. With the controlled amount of TiO_2 in the catalyst, it is possible to control the nanostructure of the catalyst. The role of Ti as an electron transfer facilitator and a supplier of hydroxide groups to the Pt surface during methanol oxidation reaction are currently investigating in our laboratory by XAS and will be addressed in future. It is also of interest to study the effect of other metal/metal oxides in improving the multi-scale dispersion in catalysts. Based on the proposed XAS structural parameters, it is possible to estimate the extent of intra-particle dispersion among the atoms in the catalyst clusters of other systems. The proposed method can produce electrocatalysts with remarkable activity for methanol oxidation with promising applications in fuel cells.

Acknowledgments

The financial support from the National Science Council (under contract numbers NSC93-2214-E-011-002, NSC93-2811-E-011-008, NSC94-2214-E-011-010, and NSC94-2120-M-011-002), the National Synchrotron Radiation Research Center (NSRRC), and the National Taiwan University of Science and Technology, Taiwan, RO.C is gratefully acknowledged.

References

[1] C. Bock, C. Paquet, M. Couillard, G.A. Botton, B.R. MacDougall, J. Am. Chem. Soc. 126 (2004) 8028.
[2] A. Dalmia, C.L. Lineken, R.F. Savinell, Colloid Interface Sci. 205 (1998) 535.
[3] L. Dubeau, C. Countanceau, E. Garnier, J.-M. Léger, C. Lamy, J. Appl. Electrochem. 33 (2003) 419.
[4] C. Bock, B.R. MacDougall, Y. LePage, J. Electrochem. Soc. 151 (2004) A1269.
[5] J.J. Rehr, R.C. Albers, Rev. Mod. Phys. 72 (2000) 621.
[6] Y.-W. Tsai, Y.-L. Tseng, L.S. Sarma, D.-G. Liu, J.-F. Lee, B.-J. Hwang, J. Phys. Chem. B 108 (2004) 8148.
[7] B.-J. Hwang, Y.-W. Tsai, L.S. Sarma, C.-H. Chen, J.-F. Lee, H.H. Strehblow, J. Phys. Chem. B 108 (2004) 15096.
[8] B.-J. Hwang, Y.-W. Tsai, L.S. Sarma, D.-G. Liu, J.-F. Lee, J. Phys. Chem. B 108 (2004) 20427.
[9] M. Watanabe, M. Uchida, S. Motoo, J. Electroanal. Chem. 229 (1987) 395.
[10] J. McBreen, S. Mukerjee, J. Electrochem. Soc. 142 (1995) 3399.
[11] M.S. Nashner, A.I. Frenkel, D.L. Adler, J.R. Shapley, R.G. Nuzzo, J. Am. Chem. Soc. 119 (1997) 7760.
[12] L.S. Sarma, T.-D. Lin, Y.-W. Tsai, J.-M. Chen, B.-J. Hwang, J. Power Sources 139 (2005) 44.
[13] B.J. Hwang, L.S. Sarma, J.M. Chen, C.H. Chen, S.C. Shih, G.R. Wang, D.G. Liu, J.F. Lee, M.T. Tang, J. Am. Chem. Soc. 127 (2005) 11140.
[14] S. Park, A. Wieckowski, M.J. Weaver, J. Am. Chem. Soc. 125 (2003) 2282.
[15] K. Kinoshita, P.N. Ross, J. Electroanal. Chem. 78 (1977) 313.
[16] H.A. Gasteiger, N. Markovic, P.N. Ross Jr., E.J. Cairns, J. Phys. Chem. 98 (1994) 617.